Preparation and characterization of nano-hydroxyapatite/polymer composite scaffolds

Xiufeng Xiao · Rongfang Liu · Qiongyu Huang

Abstract Polycaprolactone/chitosan (PCL/CS) porous composite scaffolds were prepared by solution phase separation method, and the scaffolds were further enhanced by filling with nano-hydroxyapatite/polyvinyl alcohol (n-HA/PVA) composite slurry to prepare n-HA-PVA/PCL-CS composite porous scaffolds through slurry centrifugal filling technique. The morphology, microstructure, component, porosity and mechanical property of the scaffolds were characterized using scanning electron microscope, X-ray diffraction, Fourier transform infrared spectroscope, elemental analyzer and material test machine. The results show that PCL/CS scaffolds have mutual transfixion porous structure just like honeycombs. The porosity of the scaffolds can achieve 60–80%. As the content of CS increases, the porosity increases while the compressive strength decreases. After filled with HA/PVA composite slurry, the porosity of n-HA/PCL-CS composite scaffolds decreases, but still greater than 60%, while the compression modulus can increase to 25.7 MPa.

1 Introduction

Porous hydroxyapatite ($Ca_{10}(PO_4)_6(OH)_2$, HA) has received a lot of attention for use as a bone graft material, because of its excellent resorbable and osteoconductive properties, which result from its crystallographic and chemical similarity with various calcified tissues in vertebrates [1, 2]. Nevertheless, it has not been extensively utilized, because of its brittleness and insufficient toughness [3, 4]. So much effort has been made to develop hybrid ceramic/polymer composites, in which bioactive ceramic particles are embedded into a biodegradable polymer matrix [5–9]. Using hydroxyapatite (HA) as filling material in composites is aimed at reinforcing the polymer, especially increasing its stiffness, and improving bone bonding properties of the materials, which is essential for achieving early bone in-growth and fixation of implants by bone tissues. It has been found that adding a certain amount of hydroxyapatite to the polymer matrix may turn a non-bioactive polymer into a bone-bonding composite [10–12].

Currently, polymer scaffolds have been widely used for three-dimensional (3D) cell culture to regenerate tissue-based artificial organs, including poly(α-hydroxy esters) [13], polyurethanes [14], poly(L-lactic acid) (PLLA) and poly(glycolic acid) (PGA) [15–17]. Among the available polymers, poly(ε-caprolactone) (PCL) polymer is a particularly promising material, because it undergoes auto-catalyzed bulk hydrolysis without producing any toxic by-products and possesses rubbery characteristics [18, 19]. Scaffolds based on PCL will be used in tissue engineering to carry cells or growth factors and act as templates for tissue regeneration. Hence, it seems quite beneficial to fabricate 3D porous scaffolds.

One of the most common and direct technique to prepare porous scaffolds is the particulate leaching method, which involves the casting of a polymer solution and dispersed calibrated porogen particulates in a mold, removal of the polymer solvent, followed by leaching out of the porogen [16, 20]. Because of casting and solution evaporation process, this technique is suitable for preparing thin scaffolds and residual organic solvent may be harmful to adherent cells or tissues. Freeze-dryer is also a common path to fabricate porous scaffolds. In general, freezing at a

X. Xiao · R. Liu (✉) · Q. Huang
College of Chemistry and Materials Science, Fujian Normal University, Fuzhou 350007, China
e-mail: rfliu@vip.sina.com

relatively high temperature induces a low nucleation rate and a low crystal growth rate, which leads to formation of a small number of large size solvent crystals. As a result, the average pore size obtained by freeze-drying increases when increasing freezing temperature [21, 22]. There are still many other conventional techniques to prepare porous scaffolds, such as phase separation, gas foaming, particle aggregation, which still possess disadvantages. More recently, rapid prototyping techniques involving the processing of polymer melts and powders, such as three-dimensional printing techniques [23], and fused deposition modeling [24], have received considerable interest. However, these techniques are time consuming and require sophisticated equipments. The maximal porosity obtained is limited to approximately 80%.

In this article, we used solution phase separation and slurry centrifugal filling to fabricate nano-hydroxyapatite/polymer porous scaffold. First of all, we prepared polyc-aprolactone/chitosan porous composite scaffold by means of solution phase separation. Chitosan(CS) is a rare positive charged natural alkalinous polysaccharide, possessing good biodegradability and biocompatibility together with lack of toxicity, therefore it has been widely used in the field of biomedicine [25, 26]. Because of its weak alkalinity, CS can be used in composite materials to neutralize acidic degradation products of PCL. In addition, slurry centrifugal filling technique was used to prepare HA/polymer scaffold. The slurry involved HA and polyvinyl alcohol (PVA). The reason of using PVA is that the Ca^{2+} can interact with PVA molecules to substitute intermolecular hydrogen bonds with stronger interactions [27]. The bonds between PVA and nano HA particles endow organic-inorganic composite materials with better mechanical strength. Mechanical properties and porosity of the scaffolds were characterized before and after filling with HA/PVA slurry.

2 Experiments

2.1 Materials

HA powder was prepared by hydrothermal method using $Ca(NO_3)_2 \cdot 4H_2O$, and $(NH_4)_3PO_4$ solution as reagents. The pH of $Ca(NO_3)_2$ solution was kept higher than 10.0 and that of $(NH_4)_3PO_4$ solution was kept higher than 11.0 by adding NH_3 solution. A 0.5 M solution of $Ca(NO_3)_2 \cdot 4H_2O$ containing 0.2 g polyethylene glycol was added to $(NH_4)_3PO_4$ solution, and the mixture was stirred for 0.5 h, followed with hydrothermal treatment at 200°C for 8 h. The resultant precipitates were filtered and dried at 100°C overnight.

250kD, 80-mesh chitosan (~85% deacetylated) powder was purchased from Haidebei bioengineering Co. Ltd., JiNan, China. And 70kD PCL was purchased from Daicel

chemical Co. Ltd., Japan. All the other chemicals used were of analytical degree.

2.2 Preparation of nano-HA/polymer composite scaffold

10 wt% PCL glacial acetic acid solution was prepared, then a certain amount (5–20 wt%) of CS was put into 30 g solution, and 0.5 g water was dripped into the system afterwards. The solution was stirred for 0.5 h. The mixed solution as prepared was put into 100 ml beaker to mix with 30 g 40% NaOH solution with stirring on a magnetic stirrer. When the above process was over for hours, the white scaffold was precipitated from the solution and was washed with water, as shown in Fig. 1. The scaffolds with CS contents of 5%, 10%, 15%, 20% by mass as prepared, were coded as PCS5, PCS10, PCS15, PCS20 respectively.

HA powder was dispersed into 10 wt% PVA solution by ultrasonic oscillation to prepare HA/PVA slurry(HA concentration, 5 wt%). Then the prepared PCL/CS porous scaffold was put into a tube used in centrifuge. The shape of the scaffold was 4 cm in diameter matching the tube. The slurry was put into the tube and centrifuged for 4 min at the rate of 4000 r/min. Afterwards the scaffold was taken out, dried at 40°C. The above process was repeated for 3 times. The filled scaffolds were coded as HAPCS5, HAP-CS10, HAPCS15, HAPCS20 respectively.

2.3 Porosity test

The porosity of the scaffolds was determined by a simple method [28]. To determine the porosity, different samples were washed and dried at 40°C for 1 day. After weighing (Ws), each sample was put into a pycnometer filled with ethanol, with the weight of pycnometer and ethanol taken as W1. Then the pycnometer was put into a vacuum container to extract the air out of the sample thus pushing ethanol into the space occupied by air bubble originally.

Fig. 1 The photograph of PCL/CS composite scaffold

During the vacuum process, the fluid level in the pycnometer fell down. Take out and fill up the pycnometer, then take the whole weight (W2). Afterwards, take out the sample and drip the surface ethanol back into the pycnometer to get the weight of the rest ethanol and the pycnometer (W3). The porosity can be calculated from the following equations [28], where ρ is the density of ethanol:

$$\text{Scaffold volume}: Vs = (W1 - W2 + Ws)/\rho \quad (1)$$

$$\text{Pore volume}: Vp = (W2 - W3 + Ws)/\rho \quad (2)$$

$$\text{Porosity}: \varepsilon = Vp/(Vp + Vs) = (W2 - W3 - Ws)/(W1 - W3) \quad (3)$$

2.4 Characterization of the scaffolds

The Vario EL III element analyzer was used to determine the content of C, H, O in the scaffolds. The crystal structure of prepared composites was investigated by XRD analysis. The prepared scaffolds were cut into slices and pressed into films which were then characterized by Philips X'pert MPD diffractometer using Cu $K\alpha$ generated at 40 kV and 40 mA. The samples were scanned from 10° to 90° with a step size of 0.02° and a count rate of 3.0°/min. A Nicolet Avatar 360 spectrometer was used for FTIR characterization. Signal averages were obtained for 64 scans at a resolution of 4 cm^{-1}. The samples for FTIR analysis were prepared by grinding the samples with KBr powders and then compressing the mixtures into disks. The morphology of prepared scaffolds were investigated using a Philips XL30 environmental electron microscope. The mechanical test was performed on LR5 K material test machine. The samples for the mechanical test were cut into cylinder with the diameter of 4 cm and the height of 2 cm.

3 Results and discussion

3.1 Elemental analysis of PCL/CS composite scaffold

The elemental analysis (weight percentage) of the surface of scaffolds is illustrated in Table 1. According to the percentage of N% of pure CS, we can calculate the percentage of CS in PCL/CS composite scaffolds. As shown in

Table 1, the content of CS in the scaffold is far less than expected. Therefore, the CS commingled with PCL could not be separated completely and some CS was precipitated out of the alkaline solution. Some floccus was also found in the solution.

3.2 XRD analysis

XRD patterns of PCL/CS composite scaffolds are shown in Fig. 2. There are no diffraction peaks of other substances, and all diffraction peaks are corresponding to PCL. PCL is a semi-crystalline polymer with two different peaks, around 21° and 23°. These peaks are attributed to the (110) and (200) planes [29]. With the content of CS increases, the intensity of these two peaks have a slight decrease, indicating that the addition of CS has no obvious effect on the structure of PCL, and the blending involving PCL and CS should not be the molecular-level blending. The decrease of diffraction peaks may be because that CS has positive charges, which may destroy the intermolecular interactions of PCL and its molecular regularity.

3.3 FTIR analysis

FTIR spectra of PCL, CS and PCL/CS composite scaffolds are shown in Fig. 3. The FTIR spectra of PCL and CS were compared with that of the PCL/CS composite scaffolds. The absorption bands observed in the region of 3200–3700 cm^{-1} are assigned to the O–H and N–H stretching bands of CS [30]. Compared with the spectra of PCL and CS, the absorption intensity observed in the region of 3200–3700 cm^{-1} of PCS20 is greater than that of PCS10, indicating that the content of CS in PCS20 is more than that of PCS10. The absorption peak position of composite
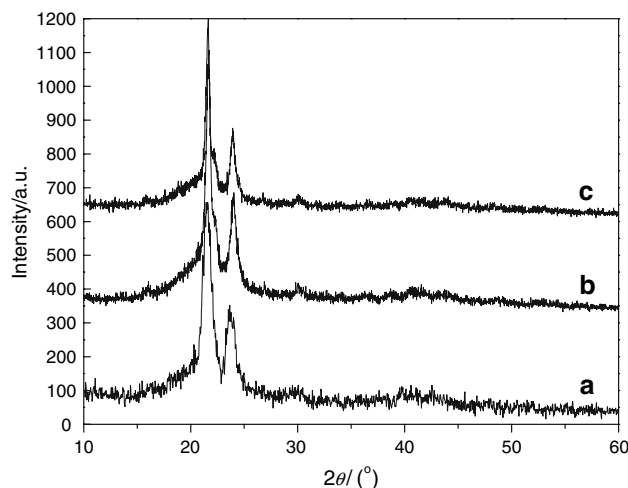
Table 1 Elemental analyses of PCL/CS composite scaffolds

Sample	C %	H %	N %	Expected CS %	Calculated CS %
PCL	63.06	8.65	–	0	0
PCS5	48.89	7.92	0.17	5	2.33
PCS15	48.25	7.99	0.47	15	6.43
PCS20	49.94	8.30	0.51	20	6.98
CS	40.59	7.18	7.31	100	100

Fig. 2 XRD analysis of PCL/CS composite scaffolds. (**a**) PCL; (**b**) PCS10; (**c**) PCS20
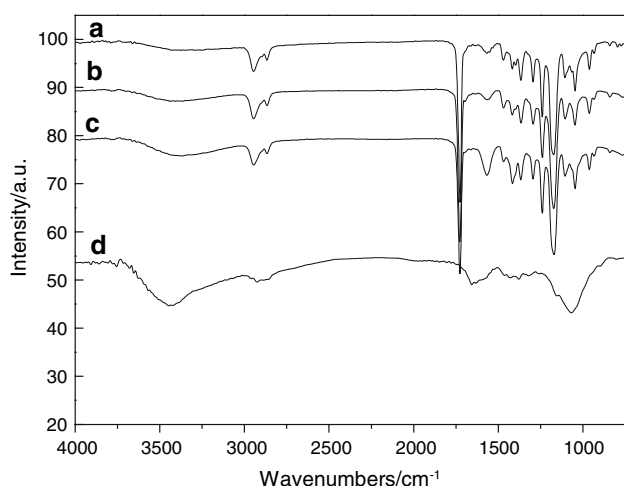
Fig. 3 FTIR spectra of the scaffolds. (**a**) PCL; (**b**) PCS10; (**c**) PCS20; (**d**) CS

scaffolds does not significantly offset, implying that there are no chemical bonds between PCL and CS.
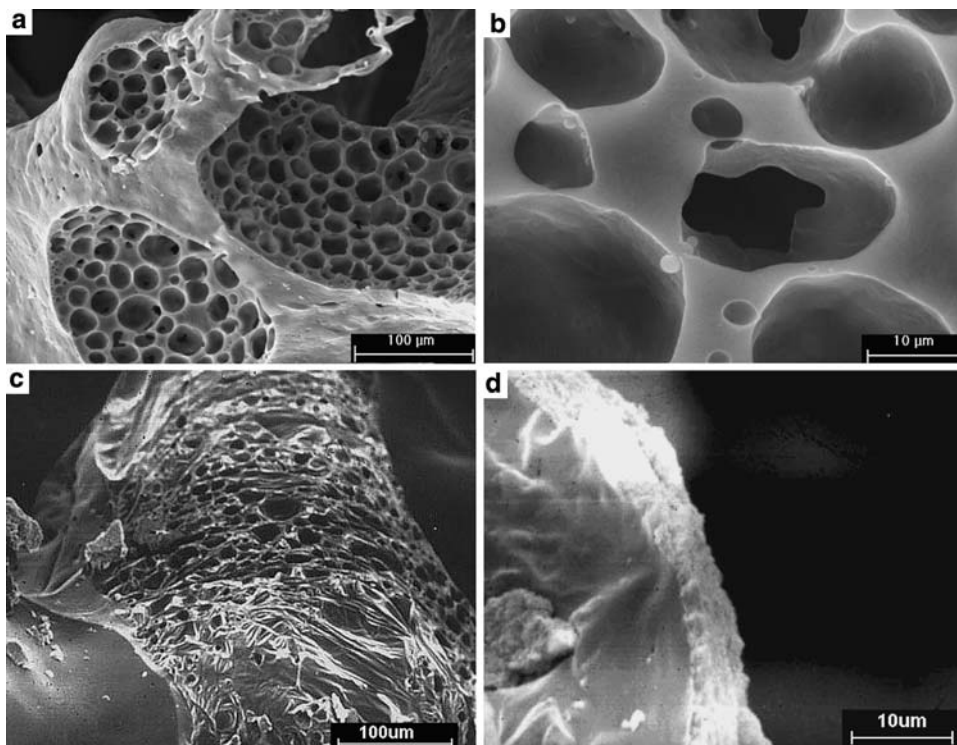
3.4 Morphology of the composite scaffolds

Figure 4a and b show SEM morphologies of PCS5 composite scaffold. It can be seen that the scaffold is formed by many interwoven PCL fibres. The scaffold contains two types of pores. One is the large pores of hundreds of microns formed by the intertwined fibres, and the other is the porous

structure like honeycombs on the surface of the fibres. The diameter of micro-pore on the fibres is about 10–40 μm. The morphology of the PCS5 after filled with only PVA slurry is shown in Fig. 4c. It is clear that the surface of fibres is covered by a bright PVA film, while after filled with HA/PVA composite slurry, the fibres are covered by a HA/PVA composite film with the thickness of about 5 μm.

Figure 5 shows the FTIR spectra of PVA, HA and PVA/HA. The peaks at 3317 cm^{-1}, 3571 cm^{-1} are the characteristics of O–H stretching bands, the peaks at 2941 cm^{-1}, 841 cm^{-1} are the characteristics of C–H stretching bands, the peak at 3317 cm^{-1} is the characteristics of O–H stretching bands and the peak at 1091 cm^{-1} belongs to C–O stretching bands. The peaks at 3449 cm^{-1} and 1638 cm^{-1} are absorption bands of water, the peaks at 1094 cm^{-1}, 1039 cm^{-1}, 960 cm^{-1}, 630 cm^{-1}, 603 cm^{-1}, 567 cm^{-1} are the characteristics of PO_4^{3-} stretching absorption bands. Compared with pure HA, the absorption peak at 1039 cm^{-1} of HA/PVA shifted to 1030 cm^{-1}, indicating that there may be chemical interactions between PO_4^{3-} and PVA. According to the studies of CHUA et al. [31], the compatibility between PVA and HA is very good. Chung and Kang et al. [27] find that HA and PVA are not simply physically blended, there should also be interactions between Ca^{2+} and PVA molecules. At the same time the hydrogen bonds between HA and PVA also cause disorder of PVA molecules. The strong interactions between HA and PVA give composite good mechanical strength.

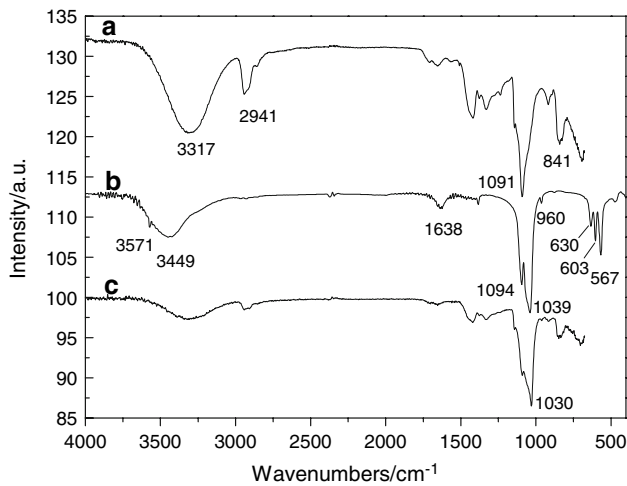**Fig. 4** SEM micrographs of the scaffolds. (**a**, **b**) PCS5; (**c**) PVA/PCS5; (**d**) HA-PVA/PCS5

Fig. 5 FTIR spectra of the materials. (**a**) PVA; (**b**) HA; (**c**) HA/PVA
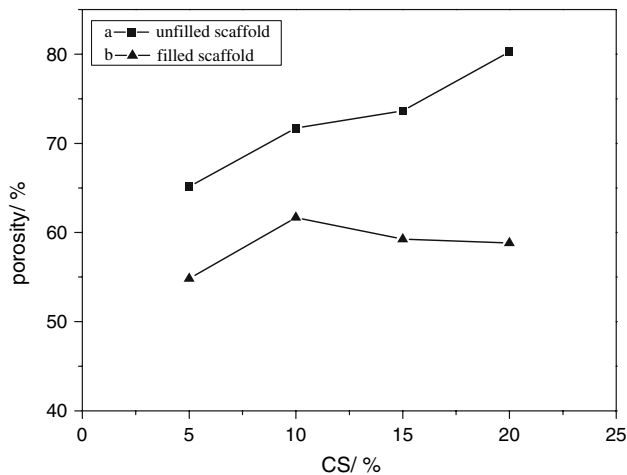
Fig. 6 Porosity the composite scaffolds. (**a**) unfilled scaffold; (**b**) filled scaffold

Fig. 7 Compressive strength of the scaffolds. PCL/CS: (**a**) PCS5; (**b**) PCS10; (**c**) PCS15; (**d**) PCS20 HA-PVA/PCL-CS: (**e**) HAPCS5; (**f**) HAPCS10; (**g**) HAPCS15; (**h**) HAPCS20

3.5 Porosity of the composite scaffolds

It can be learned from Fig. 6 that the porosity of the PCL/CS scaffolds increases as the CS content increases. CS and PCL undergo the process of swelling and dissolution in glacial acetic acid with little water. The molecular chains of CS tend to keep away from each other and intermingle with PCL molecular chains. When NaOH solution is dripped into PCL/CS blending system, PCL and CS will quickly be precipitated. Due to volume shrinking effect in the process of precipitation, the large pores are formed [28]. Because CS swells far more than PCL, the former accounts for most of the superabundant volume. The more CS is contained in the blend, the more volume occupied by CS becomes pores after CS is precipitated. When theoretical CS content reaches to 20%, the porosity is over 80%. As ca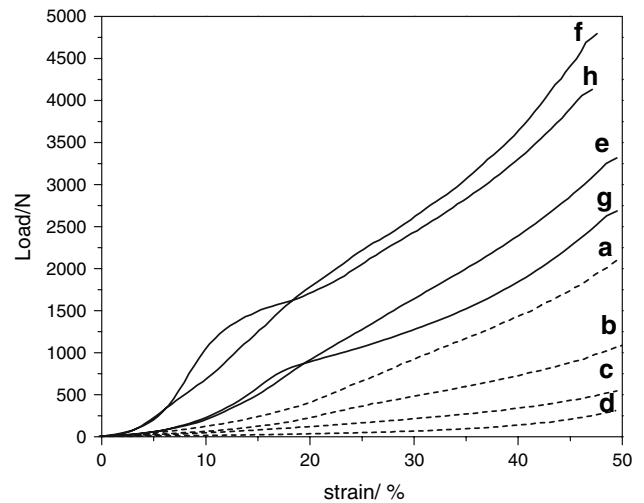n be learned from Fig. 6, the porosity of scaffolds does not decrease greatly after filling. The filled scaffolds still have a porosity of about 60%.

3.6 Mechanical test of scaffolds

The compressive strength and modulus of filled and unfilled composite scaffolds are shown in Figs. 7 and 8. As to the unfilled scaffolds, the compressive strength and the modulus decrease as the content of CS increases. As above mentioned, the porosity of the scaffolds increases as the content of CS increases. Therefore, the change of compressive strength and the modulus of the scaffolds with respect to the content of CS is relative with the porosity of the scaffolds. Compared with the unfilled scaffolds, the compressive strength and modulus of filled scaffolds are improved greatly after filled with HA/PVA slurry. As shown in Fig. 8h, the modulus of HAPCS20 can increase to 25.7 MPa.

It is noted that the modulus of unfilled scaffold (Fig. 8a–d) reaches the highest value at 20% strain, while that of filled scaffold decreases to 17%. This means that the stiffness of the scaffolds improves after filled with HA-PVA slurry. The modulus of HAPCS20 is obviously greater than that of HAPCS5, HAPCS10 and HAPCS15. The porosity of the filled scaffolds is very close, therefore, the increase of the modulus of HAPCS20 should not be ascribed to the porosity of the scaffolds. It can be inferred that the HA/PVA composite film on the fibres (Fig. 4d) plays a beneficial role in enhancing the scaffolds. The composite scaffolds are isotropy due to the random alignment of fibres. The PVA/HA composite film covering on the fibres will absorb most of the energy when the scaffolds are compressed. Further compression will cause microcracks on the brittle HA/PVA film, then the ductile fibres
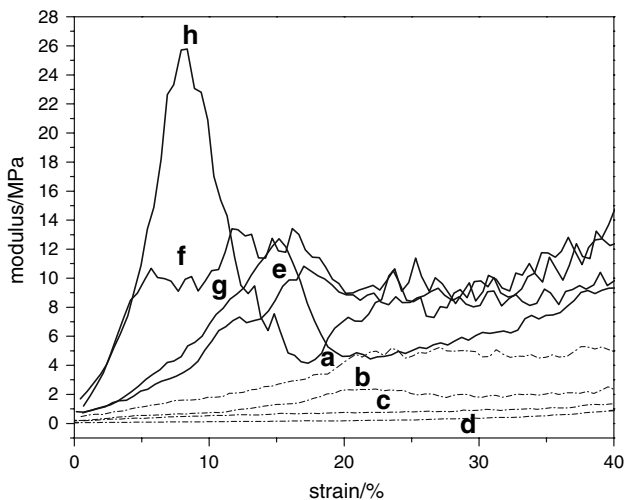
Fig. 8 Modulus-strain curves of the scaffolds. PCL/CS: (**a**) PCS5; (**b**) PCS10; (**c**) PCS15; (**d**) PCS20 HA-PVA/PCL-CS: (**e**) HAPCS5; (**f**) HAPCS10; (**g**) HAPCS15; (**h**) HAPCS20

induce a lot of silver streaks and shear bands, absorb considerable energy, thus preventing the development of micro-cracks and increasing the compressive strength and modulus of the scaffolds.

4 Conclusion

To improve the mechanical property and the bioactivity of scaffold materials for bone tissue engineering, combining the advantages of natural polymers, synthetic polymers and hydroxyapatite, PCL/CS porous composite scaffolds were prepared by solution phase separation method, and the scaffolds were further enhanced by filling with n-HA/PVA composite slurry to prepare n-HA-PVA/PCL-CS composite porous scaffolds, through slurry centrifugal filling technique. SEM observations show that PCL/CS scaffolds contain two types of pores. The porosity of PCL/CS scaffolds can achieve 60–80%. The compressive strength and modulus of the scaffolds are greatly improved after filled with HA/PVA slurry, while the porosity of the scaffolds decreases, but still greater than 60%.

References

1. M. Roy, S.K. Linnehan, Nature **247**, 220 (1974). doi:10.1038/247220a0

2. C. Lavernia, J.M. Schoenung, Am. Ceram. Soc. Bull. **70**, 95 (1991)

3. T.M.G. Chu, D.G. Orton, S.J. Hollister, S.E. Feinberg, J.W. Halloran, Biomaterials **23**, 1283 (2003). doi:10.1016/S0142-9612(01)00243-5

4. Y.H. Koh, H.W. Kim, H.E. Kim, J.W. Halloran, J. Am. Ceram. Soc. **86**, 2027 (2003). doi:10.1111/j.1151-2916.2003.tb03603.x

5. C.V.M. Rodrigues, P. Serricella, A.B.R. Linhares, R.M. Guerdes, R. Borojevic, M.A. Rossi et al., Biomaterials **24**, 4987 (2003). doi:10.1016/S0142-9612(03)00410-1

6. Y. Shikinami, M. Okuno, Biomaterials **20**, 859 (1999). doi:10.1016/S0142-9612(98)00241-5

7. R.C. Thomson, M.J. Yaszemski, J.M. Powers, A.G. Mikos, Biomaterials **19**, 1935 (1998). doi:10.1016/S0142-9612(98)00097-0

8. M.C. Azevedo, R.L. Reis, B.M. Claase, D.W. Grijpma, J. Feijen, J. Mater. Sci. Mater. Med. **14**, 103 (2003). doi:10.1023/A:1022051326282

9. G. Ciapetti, L. Ambrosio, L. Savarino, D. Granchi, E. Cenni, N. Baldini et al., Biomaterials **24**, 3815 (2003). doi:10.1016/S0142-9612(03)00263-1

10. W. Bonfield, in *Materials Characteristics Versus In Vivo Behavior*, ed. by P. Ducheyne, J.E. Lemons (New York Academy of Science, New York, 1988) p. 173

11. K.E. Tanner, C. Doyle, W. Bonfield in *Clinic Implant Materials: Advances In Biomaterials*, ed by G. Heimke, U. Soltesz, A.J.C. Lee, vol. 9 (Elsevier, Amsterdam,1990) p. 149

12. C.C.P.M. Verheyen, J.R. De Wijn, C.A. van Blitterswijk, P.M. Rozing, K. de Groot, in *Bonebonding Biomaterials*, ed. by P. Ducheyne, T. Kokubo, C.A. van Blitterswijk (Reed Healthcare Communications, Leiderdorp, The Netherlands, 1992), pp. 153–171.

13. S. Miyamoto, K. Takoaka, Ann. Chir. Gynaecol. **82**, 69 (1993)

14. F.F. Nielsen, T. Karring, S. Gogolewski, Acta. Orthop. Scand. **63**, 66 (1992)

15. A.G. Mikos, Y. Bao, L.G. Cima, DE Ingber, J.P. Vacanti, P. Langer, J. Biomed. Mater. Res. **27**, 183 (1993). doi:10.1002/jbm.820270207

16. A.G. Mikos, A.J. Thorsen, A.L. Czerwonka, Y. Bao, R. Langer, D.N. Winslow et al., Polymer (Guildf) **35**, 1068 (1994). doi:10.1016/0032-3861(94)90953-9

17. A.G. Mikos, G. Sarakinos, S.M. Leite, J.P. Vacanti, R. Langer, Biomaterials **14**, 323 (1993). doi:10.1016/0142-9612(93)90049-8

18. C.G. Pitt, F.I. Chasalow, Y.M. Hibionada, D.M. Klimas, A. Schindler, J. Appl. Polym. Sci. **26**, 3779 (1981). doi:10.1002/app.1981.070261124

19. S.A. Ali, S.P. Zhong, P.J. Doherty, D.F. Willimas, Biomaterials **14**, 648 (1993). doi:10.1016/0142-9612(93)90063-8

20. Q. Hou, D.W. Grijpma, J. Feijen, Biomaterials **24**, 1937 (2003). doi:10.1016/S0142-9612(02)00562-8

21. C. Schugens, V. Maquet, C. Grfils, R. Jerome, P. Teyssie, Polymer (Guildf) **37**, 1027 (1996). doi:10.1016/0032-3861(96)87287-9

22. R.Y. Zhang, P.X. Ma, J. Biomed. Mater. Res. **44**, 446 (1999). doi:10.1002/(SICI)1097-4636(19990315)44:4<446::AID-JBM11>3.0.CO;2-F

23. R.A. Giordano, B.M. Wu, S.W. Borl, L.G. Cima, E.M. Sachs, M.J. Cima, J. Biomater. Sci. Polym. Ed. **8**, 63 (1996). doi:10.1163/156856297X00588

24. I. Zein, D.W. Hutmacher, K.C. Tan, S.H. Teoh, Biomaterials **23**, 1169 (2002). doi:10.1016/S0142-9612(01)00232-0

25. Y. Zhang, M. Zhang, J. Biomed. Mater. Res. **55**, 304 (2001). doi:10.1002/1097-4636(20010605)55:3<304::AID-JBM1018>3.0.CO;2-J

26. L. Zhang, Y.B. Li, A.P. Yang, X.L. Peng, X.J. Wang, X. Zhang, J. Mater. Sci. Mater. Med. **16**, 213 (2005). doi:10.1007/s10856-005-6682-3

27. Y.S. Chung, S.I. Kang, O.W. Kwon, S.D. Shin, G.S. Lee, J.E. Shin, J. Appl. Polym. Sci. **106**, 3423 (2007). doi:10.1002/app.26557

28. H.D. She, X.F. Xiao, R.F. Liu, J. Mater. Sci. **42**, 8113 (2007). doi:10.1007/s10853-007-1706-7

29. Y. Chatani, Y. Okita, H. Yadokoro, Y. Yamashita, Polym. J. **1**, 555 (1970). doi:10.1295/polymj.1.555

30. F.G. Person, R.H. Marchessault, C.Y. Liang, J. Polym. Sci **43**, 101 (1960). doi:10.1002/pol.1960.1204314109

31. C.K. Chua, K.F. Leong, K.H. Tan, F.E. Wiria, C.M. Cheah, J. Mater. Sci. Mater. Med. **15**, 1113 (2004). doi:10.1023/B:JMSM.0000046393.81449.a5